DOI: 10.1002/ejoc.200900905

Keronopsamides, a New Class of Pigments from Marine Ciliates

Graziano Guella,*[a,b] Rita Frassanito[a] Ines Mancini[a] Tommaso Sandron,[a] Letizia Modeo,[c] Franco Verni,[c] Fernando Dini,[c] and Giulio Petroni[c]

Keywords: Natural products / Marine ciliates / *Pseudokeronopsis riccii* / Cortical granules / Keronopsamides / Dyes/pigments / Structure elucidation

New pigments with an unprecedented skeleton, named keronopsamides A–C, were isolated from the marine ciliate *Pseudokeronopsis riccii*. The structure of the most abundant secondary metabolite, keronopsamide A, was established through extended Nuclear Magnetic Resonance (NMR) analysis and mass spectrometric (MS) data obtained by using electrospray (ESI) and matrix assisted laser desorption (MALDI) ionizations. Structures of the minor analogues (keronopsamide B and C) were inferred from ^{1}H NMR, chemical correlation, and LC-MS measurements. The analysis of NOE dipolar couplings and quantum chemical calculations, carried out by density functional theory (DFT) on the preferred rotamers of keronopsamide A, suggested a fully planar structure with amide bond in *anti* stereochemistry capable to break down the extended conjugation of the whole π electronic system. Although the presence of a 2-substituted 3,4-dibromo-pyrrole moiety is reminiscent of previously isolated metabolites isolated from a cell extract of *Pseudokeronopsis rubra* (keronopsins), keronopsamides show a new molecular skeleton formally derived from a peptide-like condensation of a 3-pyrrolepropenoic acid with an unsaturated bromotyramine.

Introduction

Among Earth's biota, secondary metabolites are largely produced as expression of evolutionary adaptive purposes, thus characterizing often entire taxa to such a degree to represent reliable chemotaxonomic tools.[1] Our investigations of various taxa comprising the marine ciliate *Euplotes*, marked this protist as a fruitful source of new terpenoids,[2] among which euplotin C deserves particular mention being involved in several interesting biological activities.[3] Even freshwater ciliate taxa produce secondary metabolite: raw extracts of *Tetrahymena pyriformis* turned out to contain interesting polycyclic triterpenes,[4] whereas bioactive alkyl-resorcinols, referred to as "climacostol family", have been isolated from *Climacostomum virens*.[5] In this context, the photoactive phenanthroperylenequinones stentorin (**1**) and blepharismin C (**2**) (Scheme 1) isolated from the ciliates *Stentor coeruleus*[6] and *Blepharisma japonicum*[7] are also noteworthy.

These pigments have been demonstrated to act as both photoreceptors for abrupt light-avoidance responses (although the signaling cascades leading to ciliary stroke reversal still remain an intriguing issue) and defense substances, which has been inferred from their toxic effect on certain protists.[8] Toxicity of blepharismin and stentorin in the light seems to be mainly related to their capabilities to generate singlet molecular oxygen ($^1O_2$) both in situ and in the medium. More recently, a novel pigment structurally related to stentorin, called maristentorin, has been isolated from the ciliate *Maristentor dinoferus*,[9] a benthic marine species of coral reefs harbouring zooxanthellae.[10] *Stentor amethystinus* is another ciliate which produces secondary metabolites: six different mycosporine like amino acids (MAAs)[11] have been found in a single strain of this morphospecies collected from an Argentinian lake. MAAs have also been found in *M. dinoferus*[12] and in several *Chlorella*-bearing ciliates.[13]

In addition to stentorins and blepharismins, characterized by the hypericin-like skeleton, ciliate taxa comprising the cosmopolitan and ubiquitous genus *Pseudokeronopsis* (Spirotrichea, Stichotrichia)[14] produce a second class of pigments,[15] called keronopsins **3**–**6** (Scheme 1), wherein a β-bromine-substituted pyrrole is linked to a sulfate pyrone through an extended conjugated chain. In particular, keronopsins have been isolated from cell cultures of the marine morphospecies *Pseudokeronopsis rubra*.[15]

In this paper we report on the occurrence of pigments belonging to a third unrecorded class, produced by the newly described marine ciliate morphospecies, *Pseudokeronopsis riccii* (strain Oxsard2) collected from the Tyrrhenian Sea. The structural elucidation of these new pigments, named keronopsamides, are described and a possible biogenetic route for the biosynthesis of the most abundant secondary metabolite produced by *P. riccii* is given.

[a] Dipartimento di Fisica, Università di Trento, via Sommarive 14, 38100 Povo (TN), Italy
Fax: +39-0461-882009
E-mail: graziano.guella@.unitn.it
[b] Istituto di Biofisica, CNR, via alla Cascata 56/C, 38100 Povo (TN), Italy
[c] Dipartimento di Biologia, Università di Pisa, via A. Volta 4/6, 56126 Pisa, Italy

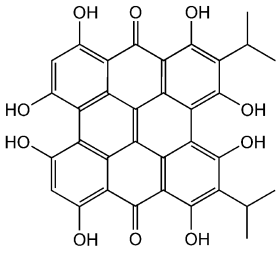

1 (stentorin)

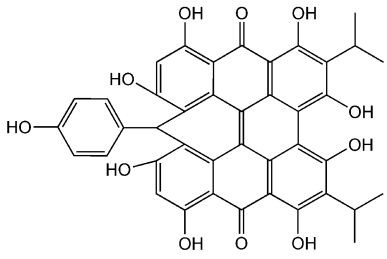

2 (blepharismin C)

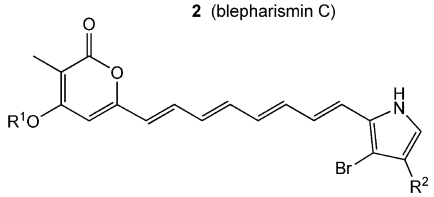

3 keronopsin A_1 $R^1 = SO_3Na$, R^2 =H
4 keronopsin A_2 $R^1 = SO_3Na$, R^2 = Br
5 keronopsin B_1 $R^1 = R^2$ = H
6 keronopsin B_2 R^1 = H, R^2 = Br

Scheme 1. Structures of pigments isolated from freshwater and marine ciliates.

Results and Discussion

The marine ciliate *Pseudokeronopsis riccii* shows an elliptical body shape (ca. 225 × 50 μm in vivo), with rounded front and rear edges, the latter slightly narrower. The cell body is very flexible and manifests a colored cortical surface owing to the presence of embedded reddish circular cortical granules ca. 1.0 μm in diameter, arranged in rosettes, small bunches, and rows docking the somatic and oral ciliature. Cytoplasm includes few scattered colored granules whose concentration does not enhance in the rear body edge, as it occurs in other species of the genus. Scattered throughout the cytoplasm other colorless, circular, cortical granules occur, ca. 1.5 μm in diameter, previously called "blood cell-shaped granules" (Figure 1).

We feel confident to exclude any symbiotic relationship of *P. riccii*, since the extensive transmission electron microscope analysis of specimens comprising the experimental strain Oxsard2 produced negative results. A detailed description of *Pseudokeronopsis riccii* will be available in a forthcoming paper (by Modeo et al.).

When the ethanol raw extract of the cells of *Pseudokeronopsis riccii* (strain Oxsard2) was subjected to liquid chromatography coupled to both Diode Array and ESI-MS detectors (HPLC-PDA-ESI/MS), the chromatogram showed one major peak strongly absorbing at 357 nm

Figure 1. In vivo photomicrograph of *Pseudokeronopsis riccii*.

[keronopsamide A (**7**)], and two minor ones corresponding to more polar metabolites absorbing at 379 nm [keronopsamides B (**8**) and C (**9**)].

The most abundant metabolite keronopsamide A (**7**) (Scheme 2) was obtained in pure form by following the standard purification procedures we recently reported for the isolation of ciliate metabolites.[2,3]

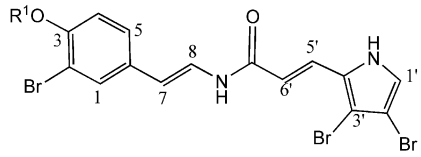

7 keronopsamide A, R^1 = H
8 keronopsamide B, $R^1 = SO_3H$

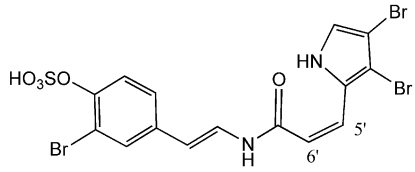

9 keronopsamide C

Scheme 2. Structures of the new alkaloids keronopsamides A (**7**), B(**8**), and C(**9**) isolated from *Pseudokeronopsis riccii*. Arbitrary numbering on structure is followed in NMR assignments (see Table 1 and Exp. Sect.)

Its molecular formula was established by MALDI-TOF and ESI-MS measurements, the latter carried out through a coupled HPLC-MS system. In the negative ion-mode MALDI spectrum of **7** a clear 1:3:3:1 quartet at the nominal masses of 487:489:491:493 was present, hence suggesting in the putative parent ion $[M - H]^-$ the presence of 3 Bromine atoms. The same 1:3:3:1 intensity pattern, although shifted of two Da (489:491:493:495), was observed in the corresponding positive ion-mode ESI spectrum in agreement with the expected parent ion as $[M + H]^+$. Moreover, the presence in the same mass spectrum of similar clusters attributable to electrostatic sodium ion adducts ($[M + Na]^+$ at *m*/*z* 511:513:515:517) and potassium ion adducts ($[M + K]^+$ at *m*/*z* 527:529:531:533), gives further support to the parent ion attribution. Finally, high resolution mass

measurements carried out by TOF analyzers (reflector mode, internal calibration) on the monoisotopic peak of the $[M - H]^-$ parent ion at *m*/*z* 487 provided the molecular composition of **7** as $C_{15}H_{11}Br_3N_2O_2$ which implies ten degrees of unsaturation. On the one hand, the analysis of 1D and 2D ^1H NMR spectra revealed the presence of i) one trisubstituted 1,2,4 benzene ring conjugated to one disubstituted carbon–carbon double bond, ii) one isolated disubstituted carbon–carbon double bond, and iii) one isolated (amide or ester) carbonyl group; on the other, ^{13}C NMR and HMBC measurements, revealed the presence of a trisubstituted pyrrole ring (δ_H 7.20 J coupled with *N*-*H* exchangeable proton at δ_H = 8.73), thus fulfilling the overall number of unsaturations. The 2-bromo-3-hydroxy phenyl moiety (arbitrary numbering as defined in Scheme 2) was established by the δ_H of aromatic protons, by their characteristic J coupling pattern (see Table 1), and by their correlation with the corresponding δ_C values from HSQC experiment. The HMBC spectrum not only confirmed this partial structure, but also allowed us to set up the substituent at position 6 as a disubstituted C(7)=C(8) double bond with *E* stereochemistry ($J_{7,8}$ = 14.7 Hz). Actually, C(7) shows ^3J hetero-correlations both with H–C(1) and H–C(5) while C(6) resulted hetero-correlated with H–C(8). However, the remaining C(5′)=C(6′) *E* double bond ($J_{5',6'}$ = 15.8 Hz) must be linked to the α position [C(4′)] of the pyrrole ring since H–C(6′) shows ^3J hetero-correlation with C(4′), whereas H–C(5′) resulted coupled to C(3′). Thus, the two moieties defined for keronopsamide A must be joined together as reported in structure **7** (Scheme 2) on the basis of the strong ^3J hetero-correlations of C(7′) with H-C(5′) on one side and with H-C(8) on the other. Taking into account the proton coupling pattern of H-C(8), the molecular formula, and the value of the ^{13}C resonance for C(7′), it was unambiguously established that the bridge between these two partial structures must be represented by an unsaturated amide bond. As additional support, the ESI(+) MS/MS fragmentation of the protonated molecular ion at the nominal mass 489 Da led to the stabilized acylium ion at the monoisotopic mass 276 Da via collision induced dissociation of the protonated amide bond (Scheme 3); as expected, this fragment ion showed the characteristic isotopic cluster as a 1:2:1 triplet due to the presence of two bromine atoms.

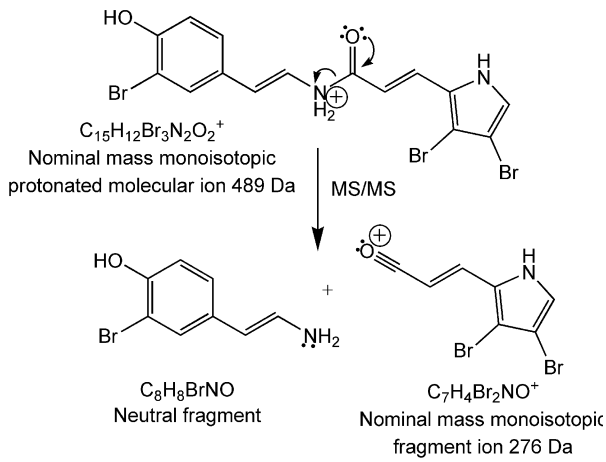

Scheme 3. The collisional activated dissociation (MS/MS) of the protonated molecular ion (ESI, positive ion mode) of keronopsamide A leading to the fragment ion at *m*/*z* 276.

The structure of the minor keronopsamide B (**8**) was established by MALDI-TOF high resolution mass spectrometric measurements and by the analysis of its ^1H NMR spectra. In particular, the molecular formula of keronopsamide B (**8**), $C_{15}H_{10}Br_3N_2O_5S$, was inferred by MALDI-TOF negative ion mass measurements, hence indicating the presence of a sulfate ester (80 Da mass shift). Remarkably, in both MALDI and ESI spectra of **8** we observed relevant losses of sulfur trioxide neutral molecules leading to the same mass spectrum previously described for **7**. The bathochromic effect on the Visible band (shifted from 358 nm in **7** to 379 nm in **8**) and NMR analysis suggest that the phen-

Table 1. NMR spectroscopic data of keronopsamide A (**7**) in CD_3COCD_3 at 298 K (^1H at 400 MHz, ^{13}C at 100 MHz).

C-Atom	δ_H (ppm), *J* [Hz]	δ_C (ppm) (HSQC)	Long-range H/C correlations (HMBC)	Relevant proton dipolar couplings (NOESY)
1	7.48 d (2.1)	130.9 d	C-3, C-5 and C-7	
2	–	111.0 s		
3	–	153.8 s		
4	6.95 d (8.6)	117.8 d	C-2, C-3 and C-6	
5	7.26 dd (2.1, 8.6)	126.5 d	C-1, C-3 and C-7	H-7
6	–	131.8 s		
7	6.16 d (14.7)	111.7 d	C-1, C-5 and C-8	H-1, H-5 and –NHCO
8	7.53 dd (10.5, 14.7)	124.0 d	C-6 and C-7′	
1′	7.20 d (3.0)	122.9 d	C-2′, C-3′ and C-4′	–
2′	–	101.5 s		
3′	–	104.4 s		
4′	–	128.2 s		
5′	7.56 d (15.4)	129.5 d	C-3′, C-6′ and C-7′	
6′	6.67 d (15.4)	118.4 d	C-4′ and C-7′	–NHCO
7′		163.9 s		
*H*O-	8.04 br. s	–		
*HN*CO-	9.55 d (10.5)	–		H-7, H-6′ and H-5′
HN-pyrrole	8.73 brd (3.0)	–		

olic OH group of **7** is esterified by sulfuric acid in structure **8** as indicated by the strong downfield effect (about 0.7 ppm) on H–C(4). The final proof was obtained by NMR observation that sulfate ester **8** afforded, in quantitative yields and fast reaction times, pure **7** when treating its deuterated methanol solution with a small amount of trichloroacetic acid; this result is in agreement with the expected hydrolytic instability of oxygen-arylsulfates in acidic media. Stereoisomeric structure **9** for keronopsamide C was ascertained mainly by its ^{1}H NMR spectrum which was almost superimposable to that of **8** with the exception for δ_H and ^3J values of H–C(5′) and H–C(6′). These protons were found as doublets ($J_{5'-6'}$ = 12.1 Hz, *Z* stereochemistry) at δ_H = 6.76 and *5.*75 respectively, in sharp contrast to the corresponding downfield doublets ($J_{5'-6'}$ = 15.6 Hz, *E* stereochemistry) at δ_H = 7.52 and 6.50 for **8**.

Tautomers and Conformational Equlibria

Due to the stabilization of the whole electronic structure of keronopsamide A through the extended π electrons conjugation, the molecule would be somehow expected to adopt an "imidic acid" tautomeric form in place of the classical "amide form" as above described for **7**. Nevertheless, structure **7** exists only in the "amide form" as firmly established by several experimental evidences. First of all, in perdeuterated dry acetone the tautomeric proton appears as a broad doublet (J_{NH-H8} = 10.3 Hz) due to the coupling of the nitrogen-linked proton with the "vicinal" H–C(8), an outcome which cannot be explained for the "imidic oxygen-linked proton" in the alternative tautomer. Furthermore, the presence in the infrared spectrum of a strong absorption at 1640 cm^{-1} is attributable to classical amide II band. Finally, the relatively low wavelength value (350 nm) of the electronic absorption is not in agreement with an extended conjugation of the whole 16 π electron system expected for the imide form. In order to understand the electronic distribution in this compound, ab initio quantum chemical calculation on both the tautomers was carried out by using Hartree–Fock level of theory followed by Density Functional (DFT) minimizations. In agreement with our experimental evidences, these calculations pointed out that **7** must exist in only one tautomeric form (amidic form). Actually, by using the 6-311G basis set, DFT calculations suggested this form at room temperature is about 18 kcal/mol more stable than the "imidic" form, thus ruling out any contribution of the latter.

Moreover, geometry minimization pointed out that keronopsamide A has a perfectly planar shape in all the stable conformers adopted by **7** following rotation of 180° around every single bond of the chain. Dipolar couplings as detected by NOESY experiments (Table 1) indicated that the amide-proton must be spatially close to H–C(7) and H–C(6′); it follows that the *anti* conformation of the amide bond must be much more populated than the *syn* conformation since the expected NOE effect between NH and H–C(6′) has not been found in the NOESY spectra of **7**. The observed NOE effects ruled out also the contributions of the conformer obtained by 180° rotation around the C8–N single bond (dihedral angle C7–C8–N–C7′ near zero) because therein a strong NOE of NH with H-8 would have been expected. On the other hand, a small contribution must be represented by conformers obtained through 180° rotation around the C6′–C7′ single bond (**7c** and **7d** in Scheme 4) because the NH amidic proton shows a small but detectable dipolar coupling with H–C(5′).

Concerning the existence of conformational isomers for rotation around the C6–C7 bond, the strong and almost equally intense NOE effects of H-7 with H-1 and H-5 speak for almost populated conformers **7a** and **7b.** Finally**,** the absence of any detectable dipolar coupling of the pyrrole NH with both H–C(5′) and H–C(6′) is a strong evidence that this proton undergoes a fast chemical exchange which hinders the occurrence of any dipolar nuclear contact.

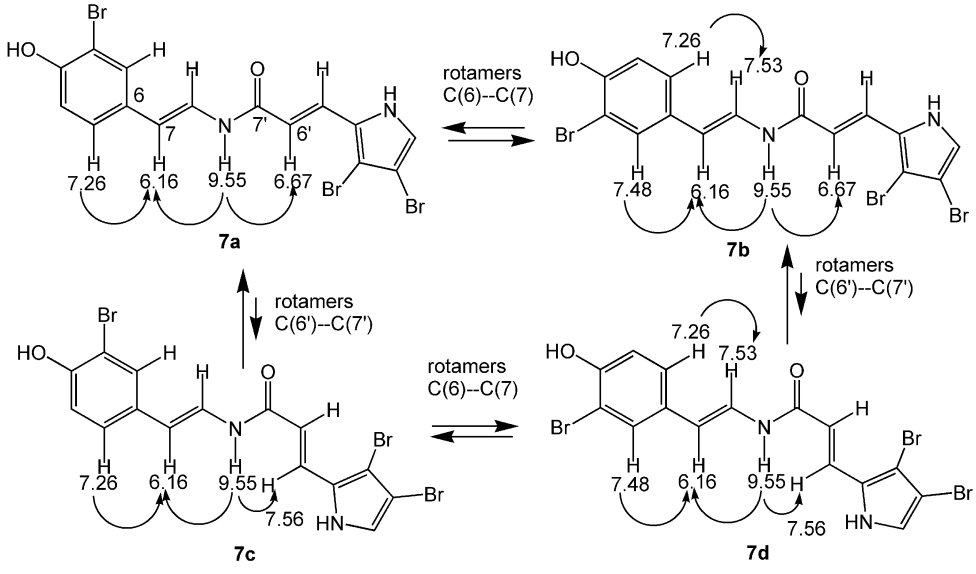

Scheme 4. Optimized geometry and conformational equilibrium of the most stable rotamers, **7a**–**7d**, of keronopsamide A.

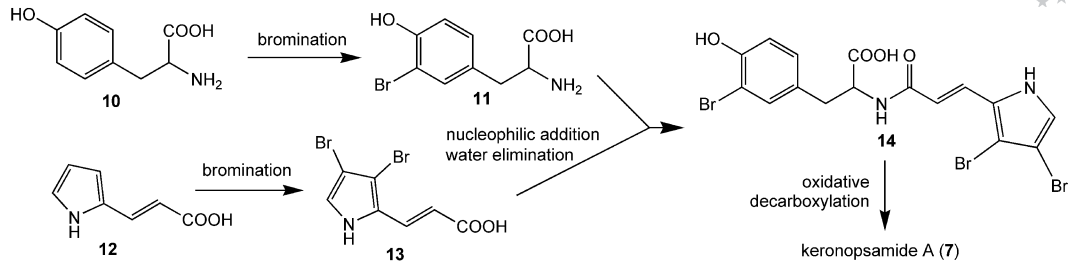

Scheme 5. Proposed biogenetic Scheme for the biosynthesis of keronopsamide A isolated from marine ciliates of the genus *Pseudokeronopsis*.

Thus, from our experimental evidences, only four conformers for keronopsamide A are present in solution (Scheme 4): the two major conformers **7a** and **7b** due to rotation around the C(6)–C(7) bond, and the two minor conformers **7c** and **7d** due to rotation around the C(6′)–C(6′) bond. The relative weight of the four rotamers was estimated by integration of the relevant NOESY maps leading to the following molar ratio **7a/7b**:(**7c+7d**) = 0.54:0.38:(0.08).

In order to obtain a theoretical evaluation of these conformational equilibria, a full conformational search was carried out at first with the molecular mechanics GMMX program[16] allowing free rotation around the C1–C7, C8–N, N–C7′, C4′–C5′, and C6′–C7′ bonds. The minimized rotamers were used as initial input structures; geometry was thereafter refined first at HF/321G, and later at DFT/B3LYP 6-31G level of theory.[17] Quantum-chemical calculations were in fair agreement with experiment results suggesting not only that conformers with amide bond in *syn* conformation were at least 5 kcal/mol higher in total energy than *anti* conformers but also that the contribution of rotamers around C8–N was negligible being at least 12 kcal/mol higher in energy than the corresponding 180° rotamers **7a-d**. Calculations supported the experimental evidences as well, pointing out a similar weight for rotamers **7a** and **7b**; in fact, two almost equally populated rotamers were evaluated by our DFT calculations (difference of total energy between **7a** and **7b**: about 0.2 kcal/mol). Finally, for the analysis of rotamers around C4′–C5′, where the experiment could not indicate any preference, calculations suggested a large prevalence (about 95%) of the conformer defined by the torsional angle NH–C4′–C5′–C6′ close to 180°.

In conclusion, NMR measurements and QM calculations suggest that keronopsamide A has an entirely planar structure and mainly exists in solution as a fast equilibrating 3:2 mixture of two C6–C7 rotamers **7a** and **7b**, as depicted in Scheme 4. According to DFT/B3LYP/6-311G+(2d,p) level of theory for **7a**, the 16 π electrons are not allowed to delocalize along the whole molecule. Even if the amide bond has a significant double bond character, the molecule appears to contain two isolated π electronic clouds, with the amide bond acting as a boundary for the extended conjugation of the π electronic system. This is somehow reflected in the Visible spectrum of keronopsamide A, which actually adsorbs at wavelengths (maximum at λ = 350 nm), lower than expected for a chromophore consisting of eight conjugated double bonds.

Biogenetic Considerations

The biosynthesis of keronopsamide A may be supposed (Scheme 5) to occur from condensation of the amine group of 3-bromotyrosine **11** (in turn derived from the electrophilic bromination of tyrosine **10**) with the β,β′-dibrominated pyrrolepropenoic acid **13** (in turn obtained by bromination of **12**), leading to the intermediate **14**. Oxidative decarboxylation of the intermediate **14** eventually provided keronopsamide A (**7**).

Conclusions

A new alkaloid pigment, keronopsamide A (**7**), and two stereoisomeric sulfate esters, keronopsamide B (**8**) and keronopsamide C (**9**), were isolated from a massive cell culture of the marine ciliate *Pseudokeronopsis riccii*. Their structures were elucidated combining the usual experimental approach relying on NMR spectroscopic data with molecular mechanics and quantum chemical calculations. Keronopsamides are the first example of secondary metabolites so far isolated from marine and freshwater ciliates belonging to a new, third class of pigments. These newly discovered secondary metabolites join the first class pigments based on the phenanthroperylenequinone skeleton (i.e. stentorins and blepharismins) and the few representatives of the second class pigments based on the keronopsin skeleton (i.e. keronopsins) already known.

The new pigments herein described are very likely localized in the cell colored cortical granules, which is in line with the localization of the other cited pigments. Moreover, any possibility of symbiont involvement in keronopsamide production could be excluded because extended TEM observation on cells did not provide any evidence of symbiotic association.

Finally, another rather interesting result of this work, which deserves consideration by both ciliatologists and natural product chemists concerning perspectives of future studies, is definitely the "secondary metabolite diversity"

discovered within the genus *Pseudokeronopsis*: actually, the two solely up to now physiologically investigated species, *P. rubra* and *P. riccii*, produce different pigments along different biogenetic routes. Studies are in progress to investigate biological activities as well as the physiological/ecological role of keronopsamides.

Experimental Section

General Methods: NMR spectra (^{1}H NMR, ^{13}C NMR, DQCOSY, NOESY, HSQC, and HMBC) for **7** were recorded on a Bruker–Avance 400 MHz NMR spectrometer by using a 5 mm BBI probe with 90° proton pulse length of 8 μs at a transmission power of 0 db. HPLC/DAD measurements were performed using a high-pressure liquid chromatograph (Hewlett–Packard model HP1100 series, Agilent Technologies Sales & Services GmbH & Co. KG, 76337 Waldbronn, Germany). A Rheodyne 7725 (Rohnert Park, CA, USA) injection valve equipped with a 20 μL internal loop for the injections was used. The analyses were performed at room temperature on a Agilent ZORBAX Eclipse XDB-C8 150 × 4.6 mm, 3.5 μm; eluent: pump A $CH_3OH/NH_4C_2H_3O_2$ 28 mM 70:30, pump B CH_3OH, gradient: 35–100% of B in 40 min, 0.8 mL min. The photodiode array (PDA) detector (Agilent 1100 series) was set at the wavelengths of 215, 254, and 450 nm. All solvents used were of analytical grade (Merck, Darmstadt, Germany) or HPLC grade (Riedel-de Haën–Sigma Chemical Co, St. Louis, MO, USA). LC/ESI-MS analysis was made on reverse phase column (Agilent Zorbax eclipse XDB-C18 4.6 × 150mm × 3.5 μm) with CH_3CN/H_2O (Riedel-de Haën) 7:3, 0.9 mL/min, split UV/MS 7/3, λ 250 nm, 5 μL injected, mounted on a Hewlett–Packard HP1100 HPLC-UV Diode Array system mated with an Esquire™ LC Bruker–Daltonics ion trap mass spectrometer. Mass spectra were obtained with an ESI source in negative-ion mode. MS conditions: source temp. 300 °C, nebulizing gas N_2, 4 L/min, positive ion mode, ISV 4 kV, OV 38.3 V, scan range 100–1000 *m*/*z*. To analyze the mass and UV the following software has been used: DataAnalysis (Version 3.0, Bruker Daltonik GmbH) and LC/MSD ChemStation (Agilent Technologies), respectively.

MALDI-TOF measurements were performed on Bruker Daltonics Ultraflex MALDI-TOF-TOF mass spectrometer equipped with a reflector unit. The acceleration voltage was set at 20 kV. For desorption of the components, a nitrogen laser beam (λ = 337 nm) was focused on the template. The laser power level was adjusted to obtain high signal-to-noise ratios, while ensuring minimal fragmentation of the parent ions. All measurements were carried out in the delayed extraction mode, allowing the determination of monoisotopic mass values (*m*/*z*; mass-to-charge ratio). After crystallization at ambient conditions, both positive and negative ion spectra were acquired in the reflectron mode, giving mainly singly protonated molecular ions ($[M + H]^+$) or sodiated adducts ($[M + Na]^+$) and deprotonated molecular ions ($[M - H]^-$), respectively. Samples were directly applied onto the stainless-steel spectrometer plate as 1 μL droplets, followed by the addition of 1 μL of DHB-matrix solution (0.5 M of 2,5-DHB in methanol containing 0.1% TFA). Every mass spectrum represents the average of about 100 single laser shoots.

Infrared spectra were recorded by using a FT-IR Equinox 55 Bruker spectrometer (ATR configuration) at 1 cm^{-1} resolution in the absorption region $\Delta\tilde{\nu}$ 4000–1000 cm^{-1}. A thin solid layer is obtained by evaporation of a methanol solution of keronopsamide A. The instrument was purged with a constant dry air flux and clean ATR crystal as background was used. Spectra processing was made using Opus software package.

Molecular mechanics calculations were carried out by the computer program GMMX as implemented in PCMODEL 7.0.[16] All the minimized structures falling in a strain-energy window of 3.0 kcal/mol were saved and finally minimized with both MMX and MM3 force fields keeping only those falling in a 2.0 kcal/mol.

Ab initio calculations were performed with the Gaussian 03 program suite[17] utilizing unrestricted hybrid density functional/molecular orbital theory with a Lee–Yang–Parr correlation functional[18] a Becke 3-parameter exchange functional (for example, B3LYP)[19] and basis sets of 6-311+G(d,p).[20]

Ciliate Strain Collection, Culturing, and Isolation of the Metabolites: *Pseudokeronopsis riccii* (Spirotrichea, Stichotrichia) is a new species whose formal description using a multidisciplinary approach (morphological-ultrastructural description plus 18S rRNA gene sequencing) will be elsewhere reported (Modeo et al., in preparation). A monoaxenic culture of the clonal strain Oxsard2 was established under laboratory conditions since spring 1999. A single specimen was isolated separately from a naturally occurring *P. riccii* population, sampling marine tidal pools (1–2 m deep) along the Tyrrhenian coast of Sardinia, near "Torre di Piscinni" (Cagliari, Italy, N 38° 54′ 15.57", E 8° 46′ 40.67′′). The analytical, clonal, massive cultures were grown by feeding them twice a week on a clonal line of the diatom *Pheodactylym tricornutum* (culture medium, 33 ‰ salinity) and maintained in a laboratory incubator at 19 ± 1 °C in a 12 h light/dark regimen (200 μmol photons $m^{-2}s^{-1}$). The massive cultures (ca. 2×10^6 cells per liter) were frequently cleaned by means of filtering (diameter of the gauze pores: 100 μm) and bimonthly processed for secondary metabolite extraction as hereby described. After a 5–7 d starving period, cells of 5–7 liter massive cultures were harvested through the following two step pelletting procedure at room temperature: 1. some preliminary centrifugations at 200 *g* to lower the massive cultures to ca. 200 mL without endangering the cells; 2. a single last centrifugation at 920 *g* to reach a pellet varying from 0.3 to 0.6 mL. Then, cells were suspended in absolute ethanol and stored at –20 °C. Through the massive culturing up to 2.9 mL of closely packed, ethanol preserved ciliates (ca. 5×10^7 cells) were obtained for the secondary metabolite analysis. Cells concentrated by filtration were extracted by ethanol at room temperature. The extraction was repeated until the glass filter appeared colorless, then the extracts were combined, reduced to dryness by rotary evaporation and then partitioned between ethyl acetate and water. Organic extract was initially purified by flash-chromatography [RP-18 LiChroCART250-4 (5 μm Merck), acetonitrile/water gradient elution]. Metabolites of interest, contained in fractions 4–6 and 10–14 were further purified by HPLC (Si-60 Merck LiChrosphere CN column, *n*-hexane/*i*PrOH, gradient elution), giving pure **7** (t_R = 7.6 min, 1.8 mg). Keronopsamide B (**8**) and keronopsamide C (**9**) were obtained in almost pure form by using RP-HPLC (Merck Lichrosphere RP18), gradient elution with acetonitrile/ water from 3:7 to 7:3 in 30 min (t_R = 5.1 min, 0.1 mg for **8**, and t_R = 11.8 min, 0.2 mg for **9**). In the same chromatographic conditions the retention time of keronopsamide A (**7**) is 18.1 min.

Keronopsamide A (7): Yellow amorphous solid. NMR spectroscopic data (see Table 1, solvent: [D_6]acetone). ^{1}H NMR (CD_3OD): δ = 7.90 (s, 1 H, NHCO), 7.50 (d, $^3J_{5',6'}$ = 15.8 Hz, 1 H, 5′-H), 7.44 (d, $J_{1,5}$ = 2.1 Hz, 1 H, 1-H), 7.43 (d, $^3J_{7,8}$ = 14.7 Hz, 1 H, 8-H), 7.19 (dd, $J_{1,5}$ = 2.1, $J_{4,5}$ = 8.5. Hz 1 H, 5-H), 7.04 (s, 1′-H), 6.83 (d, $J_{4,5}$ = 8.5 Hz, 1 H, 4-H), 6.49 (d, $^3J_{5',6'}$ = 15.8 Hz, 1 H, 6′-H), 6.18 (d, $^3J_{7,8}$ = 14.7 Hz, 1 H, 7-H) ppm. ^{13}C NMR (CD_3OD): δ = 165.8 (s, NHCO), 154.2 (s, C-3), 131.8 (s, C-6), 131.2 (d, C-1), 131.1 (d, C-5′), 127.7 (s, C-4′), 126.5 (d, C-5), 123.1 (d, C-8), 122.8 (d,

C-1′), 117.8 (d, C-4), 116.6 (d, C-6′), 113.6 (d, C-7), 111.1 (s, C-2), 105.1 (s, C-3′), 101.5 (s, C2′) ppm. FT-IR (neat): $\tilde{\nu}$ = 3420 (strong, NH and OH stretching), 1683 (strong, C=O stretching) cm^{-1}. UV (MeOH): λ_{max} (ε) = 357 nm (29100 $mol^{-1} dm^3 cm^{-1}$) MALDI-TOF (negative ion mode) HR-MS: *m/z* 486.8220 ± 0.010 (calcd. for $C_{15}H_{11}Br_3N_2O_2$: 486.8298). ESI-MS (positive ion mode detection) *m/z*: $[M + H]^+$ $[M + Na]^+$ and $[M + K]^+$ as 1:3:3:1 quartets at nominal masses 489:491:493:495, 511:513:515:517 and 527:529:531:533, respectively. ESI-MS (negative ion mode detection) *m/z*: $[M - H]^-$ as 1:3:3:1 quartet at nominal masses 487:489:491:493.

Keronopsamide B (8): ^1H NMR (CD_3OD): δ = 7.57 (d, $J_{1,5}$ = 2.1 Hz, 1 H, 1-H), 7.56 (d, $^3J_{7,8}$ = 14.7 Hz, 1 H, 8-H), 7.52 (d, $^3J_{5',6'}$ = 15.8 Hz, 1 H, 5′-H), 7.51 (d, $J_{4,5}$ = 8.5 Hz, 1 H, 4-H), 7.30 (dd, $J_{1,5}$ = 2.1, $J_{4,5}$ = 8.5. Hz 1 H, 5-H), 7.04 (s, 1′-H), 6.50 (d, $^3J_{5',6'}$ = 15.8 Hz, 1 H, 6′-H), 6.18 (d, $^3J_{7,8}$ = 14.7 Hz, 1 H, 7-H) ppm. UV (MeOH): λ_{max} (ε) = 379 nm (31000 $mol^{-1} dm^3 cm^{-1}$). ESI-MS (negative ion mode detection) *m/z*: $[M - H]^-$ and $[M - SO_3 - H]^-$ as 1:3:3:1 quartets at nominal masses 567:569:571:573 and 487:489:491:493, respectively. Compound **8** afforded pure **7** when treated in NMR tube (CD_3OD) with a catalytic amount of trichloroacetic acid.

Keronopsamide C (9): ^1H NMR (CD_3OD): δ = 7.56 (d, $^3J_{7,8}$ = 14.7 Hz, 1 H, 8-H), 7.54 (d, $J_{1,5}$ = 2.1 Hz, 1 H, 1-H), 7.50 (d, $J_{4,5}$ = 8.5 Hz, 1 H, 4-H), 7.30 (dd, $J_{1,5}$ = 2.1, $J_{4,5}$ = 8.5. Hz 1 H, 5-H), 7.04 (s, 1′-H), 6.76 (d, $^3J_{5',6'}$ = 12.1 Hz, 1 H, 5′-H), 5.75 (d, $^3J_{5',6'}$ = 12.1 Hz, 1 H, 6′-H), 6.18 (d, $^3J_{7,8}$ = 14.7 Hz, 1 H, 7-H) ppm. ESI-MS (negative ion mode detection) *m/z*: $[M - H]^-$ and $[M - SO_3 - H]^-$ as 1:3:3:1 quartets at nominal masses 567:569:571:573 and 487:489:491:493, respectively.

Supporting Information (see also the footnote on the first page of this article): 400 MHz NMR (CD_3COCD_3) spectra of keronopsamide A **7**. ^1H NMR (Figure S1), COSY full spectrum (Figure S2), HSQC (Figure S3), HMBC (Figure S4), and NOESY (Figure S5).

Acknowledgments

This research was supported by the Italian Department of Environment (Ministero dell'Ambiente e della Tutela del Territorio e del Mare), projects DPN-2008-005185 and 27/02/08-21/12/07. Additional support was provided by funds of University of Trento, Department of Physics and University of Pisa, Department of Biology.

[1] J. C. Frisvad, B. Andersen, U. Thrane, *Mycol. Res.* **2008**, *112*, 231–240.

[2] a) F. Dini, G. Guella, P. Giubbilini, I. Mancini, F. Pietra, *Naturwissenschaften* **1993**, *80*, 84–86; b) G. Guella, F. Dini, A. Tomei, F. Pietra, *J. Chem. Soc. Perkin Trans. 1* **1994**, *2*, 161–166; c) G. Guella, F. Dini, F. Erra, F. Pietra, *J. Chem. Soc., Chem. Commun.* **1994**, *22*, 2585–2586; d) G. Guella, F. Dini, F. Pietra, *Helv. Chim. Acta* **1995**, *78*, 1747–1754; e) G. Guella, F. Dini, F. Pietra, *Helv. Chim. Acta* **1996**, *79*, 710–717; f) G. Guella, F. Dini, F. Pietra, *Helv. Chim. Acta* **1996**, *79*, 2180–2189; g) G. Guella, F. Dini, F. Pietra, *Helv. Chim. Acta* **1996**, *79*, 439–448; h) G. Guella, F. Dini, F. Pietra, *Angew. Chem.* **1999**, *111*, 1217–1220; *Angew. Chem. Int. Ed.* **1999**, *38*, 1134–1136; i) G. Guella, E. Callone, I. Mancini, G. Uccello-Barretta, F. Balzano, F. Dini, *Eur. J. Org. Chem.* **2004**, *6*, 1308–1317; j) G. Guella, E. Callone, G. Di Giuseppe, R. Frassanito, F. Frontini, I. Mancini, F. Dini, *Eur. J. Org. Chem.* **2007**, *31*, 5226–5234.

[3] a) D. Savoia, C. Avanzini, T. Allice, E. Callone, G. Guella, F. Dini, *Antimicrob. Agents Chemother.* **2004**, *48*, 3828–3833; b) D. Cervia, D. Martini, M. Garcia-Gil, G. Di Giuseppe, G. Guella, F. Dini, P. Bagnoli, *Apoptosis* **2006**, *11*, 829–843; c) D. Cervia, M. Garcia-Gil, E. Simonetti, G. Di Giuseppe, G. Guella, P. Bagnoli, F. Dini, *Apoptosis* **2007**, *12*, 1349–1363; d) P. Ramoino, C. Usai, S. Maccione, F. Beltrame, A. Diaspro, M. Fato, G. Guella, F. Dini, *Aquat. Toxicol.* **2007**, *85*, 67–75.

[4] I. Abe, M. Rohmer, *J. Chem. Soc., Chem. Commun.* **1991**, 902–903.

[5] M. E. Masaki, T. Harumoto, M. N. Terazima, A. Miyake, Y. Usuki, H. Iio, *Tetrahedron Lett.* **1999**, *40*, 8227–8229.

[6] N. Tao, M. Orlando, J. Hyon, M. Gross, P. Song, *J. Am. Chem. Soc.* **1993**, *115*, 2526–2528.

[7] a) G. Checcucci, R. S. Shoemaker, E. Bini, R. Cerny, N. Tao, J. Hyon, D. Gioffre, F. Ghetti, F. Lenci, P. Song, *J. Am. Chem. Soc.* **1997**, *119*, 5762–5763; b) M. Maeda, H. Naoki, T. Matsuoka, Y. Kato, H. Kotsuki, K. Utsumi, T. Tanaka, *Tetrahedron Lett.* **1997**, *38*, 7411–7414; c) D. Spitzner, G. Höfle, I. Klein, S. Pohlan, D. Ammermann, L. Jaenicke, *Tetrahedron Lett.* **1998**, *39*, 4003–4006.

[8] a) M. E. Masaki, S. Hiro, Y. Usuki, T. Harumoto, M. N. Terazima, F. Buonanno, A. Miyake, H. Iio, *Tetrahedron* **2004**, *60*, 7041–7048; b) Y. Muto, T. Matsuoka, A. Kida, Y. Okano, Y. Kirino, *FEBS Lett.* **2001**, *508*, 423–426.

[9] P. Mukherjee, D. B. Fulton, M. Halder, X. Han, D. W. Armstrong, J. W. Petrich, C. S. Lobban, *J. Phys. Chem. B* **2006**, *110*, 6359–6364.

[10] a) C. S. Lobban, M. Schefter, A. G. B. Simpson, X. Pochon, J. Pawlowski, W. Foissner, *Mar. Biol.* **2002**, *140*, 411–423; b) C. S. Lobban, M. Schefter, A. G. B. Simpson, X. Pochon, J. Pawlowski, W. Foissner, *Mar. Biol.* **2002**, *141*, 207–208; c) W. Miao, A. G. B. Simpson, C. Fu, C. S. Lobban, *J. Eukaryot. Microbiol.* **2005**, *54*, 11–15.

[11] B. Tartarotti, G. Baffico, P. Temporetti, H. E. Zagarese, *J. Plankton Res.* **2004**, *26*, 753–762.

[12] R. Sommaruga, K. Whitehead, J. M. Shick, C. S. Lobban, *Protist* **2006**, *157*, 185–191.

[13] B. Sonntag, M. Summerer, R. Sommaruga, *Freshwater Biol.* **2007**, *52*, 1476–1485.

[14] a) H. Berger, *Monograph of the Urostyloidea (Ciliophora, Hypotricha)*. Monographiae Biologicae, H. J. Dumont (Eds.), Springer, **2006**, Vol. 85; b) X. Hu, W. Song, *Acta Protozool.* **2001**, *40*, 107–115; c) X. Hu, A. Warren, T. Suzuki, *Acta Protozool.* **2004**, *43*, 351–368; d) W. Lueken, G. Uhlig, T. Kruppel, *J. Protozool.* **1989**, *36*, 350–353; e) X. Shi, X. Hu, A. Warren, G. Liu, *Acta Protozool.* **2007**, *46*, 41–54; f) W. Song, N. Wilbert, A. Warren, *Acta Protozool.* **2002**, *41*, 145–162; g) W. Song, A. Warren, D. Roberts, N. Wilbert, L. Li, S. Ping, X. Hu, H. Ma, *Acta Protozool.* **2002**, *45*, 271–287; h) R. C. Wanick, I. D. Silva-Neto, *Zootaxa* **2004**, *587*, 1–11; i) E. Wirnsberger, H. F. Larsen, G. Uhlig, *Eur. J. Protistol.* **1987**, *23*, 76–88; j) Z. Yi, Z. Chen, A. Warren, D. Roberts, K. A. S. Al-Rasheid, M. Miao, S. Gao, C. Shao, W. Song, *J. Zool.* **2008**, *275*, 268–275.

[15] G. Höfle, S. Pohlan, G. Uhlig, K. Kabbe, D. Schumacher, *Angew. Chem. Int. Ed. Engl.* **1994**, *33*, 1495–1497.

[16] PCMOD 7.0/GMMX version 1.5, Serena Software, P. O. Box 3076, Bloomington.

[17] M. J. Frisch, G. W. Trucks, H. B. Schlegel, G. E. Scuseria, M. A. Robb, J. R. Cheeseman, J. A. Montgomery, T. Vreven, K. N. Kudin, J. C. Burant, J. M. Millam, S. S. Iyengar, J. Tomasi, V. Barone, B. Mennucci, M. Cossi, G. Scalmani, N. Rega, G. A. Petersson, H. Nakatsuji, M. Hada, M. Ehara, K. Toyota, R. Fukuda, J. Hasegawa, M. Ishida, T. Nakajima, Y. Honda, O. Kitao, H. Nakai, M. Klene, X. Li, J. E. Knox, H. P. Hratchian, J. B. Cross, C. Adamo, J. Jaramillo, R. Gomperts, R. E. Stratmann, O. Yazyev, A. J. Austin, R. Cammi, C. Pomelli, J. W. Ochterski, P. Y. Ayala, K. Morokuma, G. A. Voth, P. Salvador, J. J. Dannenberg, V. G. Zakrzewski, S. Dapprich, A. D. Daniels, M. C. Strain, O. Farkas, D. K. Malick, A. D. Rabuck, K. Raghavachari, J. B. Foresman, J. V. Ortiz, Q. Cui, A. G. Baboul, S. Clifford, J. Cioslowski, B. B. Stefanov, G. Liu, A. Lia-

shenko, P. Piskorz, I. Komaromi, R. L. Martin, D. J. Fox, T. Keith, M. A. Al-Laham, C. Y. Peng, A. Nanayakkara, M. Challacombe, P. M. W. Gill, B. Johnson, W. Chen, M. W. Wong, C. Gonzalez, J. A. Pople, *Gaussian 03*, *Revision C.02*, Gaussian, Inc., Wallingford CT, **2004**.
[18] C. Lee, W. Yang, R. G. Parr, *Phys. Rev. B* **1988**, *37*, 785–789.
[19] a) A. D. Becke, *J. Chem. Phys.* **1993**, *98*, 5648–5652; b) B. Mielich, A. Savin, H. Stoll, H. Preuss, *Chem. Phys. Lett.* **1989**, *157*, 200–206.
[20] a) R. Krishnan, J. S. Binkley, R. Seeger, J. A. Pople, *J. Chem. Phys.* **1980**, *72*, 650–654; b) T. Clark, J. Chandrasekhar, G. W. Spitznagel, P. v. R. Schleyer, *J. Comput. Chem.* **1983**, *4*, 294–301; c) A. D. McLean, G. S. Chandler, *J. Chem. Phys.* **1980**, *72*, 5639–5648.

Received: August 10, 2009
Published Online: December 3, 2009

